Pergamon

Materials Research Bulletin 37 (2002) 605–615

Materials Research Bulletin

# Crystal structure and microwave dielectric properties of $(1 - x)NdAlO_3$–$xCaTiO_3$ ceramics

Min-Han Kim[a], Chang-Soo Woo[a], Sahn Nahm[a,*], Chang-Hack Choi[b], Hwack-Joo Lee[c], Hyun-Min Park[c]

[a]*Department of Materials Science and Engineering, Korea University, 1-5 Ka, Anam-Dong, Sungbuk-Ku, Seoul 136-701, South Korea*
[b]*Advanced Materials Technology, 17-2 Jamwon-Dong, Seocho-Ku, Seoul 137-030, South Korea*
[c]*New Materials Evaluation Center, Korea Research Institute of Standards and Science, Taeduk Science Town, Taejon 305-600, South Korea*

(Refereed)
Received 20 November 2000; received in revised form 8 May 2001; accepted 17 August 2001

**Abstract**

Crystal structure and microwave dielectric properties of $(1 - x)NdAlO_3$–$xCaTiO_3$ ceramics have been investigated. Crystal structure of the specimens changed with the composition. Rhombohedral structure was found for the specimens with $x \leq 0.1$. When $0.3 \leq x \leq 0.7$, the specimens had the tetragonal structure and it changed to the orthorhombic structure as $x$ exceeded 0.7. Two types of the second phases were observed in $(1 - x)NdAlO_3$–$xCaTiO_3$ ceramics. For the specimens with $x \leq 0.5$, $Nd_4Al_2O_9$ phase was observed and Al-rich phase was found in the specimens with $x \geq 0.7$. The dielectric constant ($\varepsilon_r$) and the temperature coefficient of the resonant frequency ($\tau_f$) increased with the increase of $x$. The $Q \times f$ value of the specimen increased with $x$ and exhibited the maximum value when $x = 0.5$. The microwave dielectric properties of $Q \times f = 45{,}000$ GHz, $\varepsilon_r = 45$ and $\tau_f = -1.5$ ppm/°C were obtained for $0.3NdAlO_3$–$0.7CaTiO_3$ ceramics. 

*Keywords:* A. Ceramics; A. Electronic materials; C. X-ray diffraction; D. Dielectric properties

## 1. Introduction

Microwave dielectric materials of a high quality factor ($Q$-value), a good stability of temperature coefficient of resonant frequency and a high dielectric constant have

* Corresponding author. Fax: +82-2-928-3584.
*E-mail address:* snahm@korea.ac.kr (S. Nahm).

0025-5408/02/$ – see front matter 
PII: S0025-5408(01)00793-0

been extensively studied because of their applications to microwave devices [1,2]. Many investigations were carried out on the materials with a high dielectric constant such as $BaO–Re_2O_3–TiO_2$ (Re = rare earth) and (Pb, Ca)$ZrO_3$ systems [3–5]. The complex perovskite materials with a low dielectric constant and a high $Q$-value were also intensively studied [6–8]. Recently, the interests on the dielectric materials with a intermediate dielectric constant ($\varepsilon_r \geq 45$) and a high $Q \times f$ value (>43,000 GHz) have been increased. (Zr, Sn)$TiO_4$ ($Q \times f = 45{,}000$ GHz, $\varepsilon_r = 38$) ceramics is known to have a high quality factor but the dielectric constant is relatively low [9]. The $(1-x)LaAlO_3$–$x$Ca(or Sr)$TiO_3$ system has been investigated and the microwave dielectric properties of $Q \times f = 47{,}000$ GHz, $\varepsilon_r = 38$ and $\tau_f = 5$ ppm/°C were obtained for $0.35LaAlO_3$–$0.65CaTiO_3$ ceramics [10,11]. The $Q$-value of $0.35LaAlO_3$–$0.65CaTiO_3$ ceramics is high but the dielectric constant is still low. The microwave dielectric properties of $(1-x)La(Zn_{0.5}Ti_{0.5})O_3$–$x$Ca(or Sr)$TiO_3$ system were also studied but the results were not satisfactory [12,13].

According to the previous work, $NdAlO_3$ has a rhombohedral structure and the dielectric properties of $NdAlO_3$ are similar to those of $LaAlO_3$ [14,15]. Therefore, if $CaTiO_3$ were incorporated to $NdAlO_3$, it would be possible to develop a dielectric material which has an intermediate value of dielectric constant and a high $Q$-value. The objective of this work is to investigate the crystal structure and the microwave dielectric properties of $(1-x)NdAlO_3$–$xCaTiO_3$ ceramics and to find a new materials with $\varepsilon_r \geq 45$, $Q \times f > 43{,}000$ GHz and $\tau_f$ of zero.

## 2. Experimental

The starting materials were $Nd_2O_3$, $Al_2O_3$, $CaCO_3$, and $TiO_2$. They were mixed for 24 h in nylon jar with $ZrO_2$ balls, and then dried and calcined at 1200–1400°C for 10 h. After remilling, the powder was dried and pressed into disk and sintered at 1420–1600°C for 6 h in air. Phase identification of the specimen was carried out using a Rigaku D/max-B diffractometer with a conventional Cu Kα radiation. Lattice parameters were calculated by least-square refinement of data collected with an internal Si standard. TREOR was used for least-square refinement. The microstructure of the specimens was studied by using scanning electron microscopy (SEM) (Hitach S-4300). The density of the sintered specimens was measured by water-immersion technique. The dielectric properties in the microwave frequency range were measured by a dielectric post resonator technique suggested by Hakki and Coleman [16] and Courtney [17]. The temperature coefficient of the resonant frequency was measured at 5 GHz in the temperature range of 25–85°C.

## 3. Results and discussion

Fig. 1 shows the X-ray diffraction patterns of $(1-x)NdAlO_3$–$xCaTiO_3$ ceramics with $0.0 \leq x \leq 0.9$ sintered at 1450°C. All the peaks were indexed in terms of the

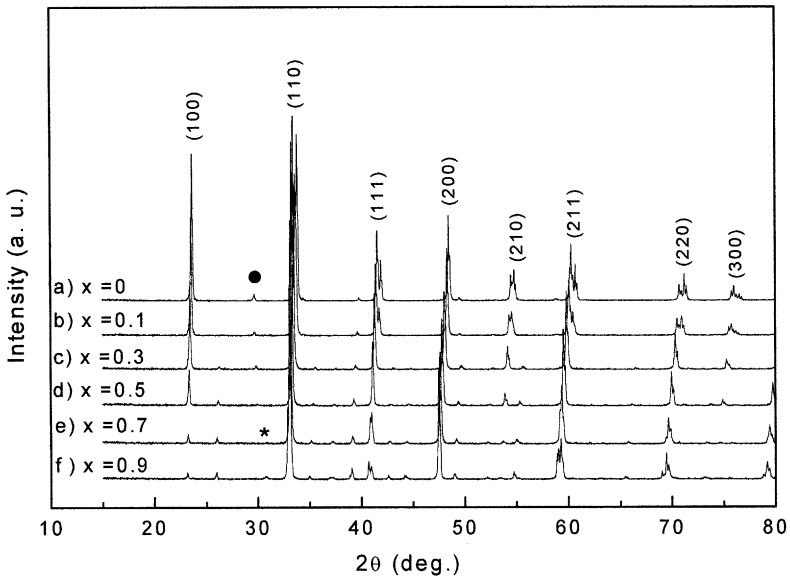


Fig. 1. X-ray diffraction patterns of $(1-x)NdAlO_3$–$xCaTiO_3$ ceramics with $0.0 \leq x \leq 0.9$ sintered at 1450°C.

simple perovskite unit cell. Two types of the second phases were observed in $(1-x)NdAlO_3$–$xCaTiO_3$ ceramics. For the specimens with $x \leq 0.5$, the peak for the $Nd_4Al_2O_9$ second phase indicated by full circle was found. The intensity of the peak for $Nd_4Al_2O_9$ phase decreased with the increase of $x$ and disappeared for specimens with $x > 0.5$. When $x$ exceeded 0.5, the peak for the unknown phase indicated by the asterisk was found and the intensity of the peak increased with the $x$. In addition, the peak for the chemical ordering was not observed in these specimens.

The shape of the X-ray peaks changed with $x$ [see the (220) peak] implying the variation of the crystal structure with the composition. In order to find the crystal structure of the specimens, the lattice parameters of the specimens were calculated from the X-ray diffraction patterns and the results are illustrated in Table 1. Silicon was

Table 1
Lattice parameters of $(1-x)NdAlO_3$–$xCaTiO_3$ ceramics

| Composition | Lattice parameters (Å) | | | $\alpha = \beta = \gamma$ | Structure |
|---|---|---|---|---|---|
| | $a$ | $b$ | $c$ | | |
| $x = 0.0$ | 3.7522 | – | – | 90.355 | Rhombohedral |
| $x = 0.1$ | 3.7642 | – | – | 90.330 | Rhombohedral |
| $x = 0.3$ | 5.3470 | – | 7.5760 | 90 | Tetragonal |
| $x = 0.5$ | 5.3770 | – | 7.5930 | 90 | Tetragonal |
| $x = 0.7$ | 5.4000 | – | 7.6250 | 90 | Tetragonal |
| $x = 0.9$ | 5.4320 | 5.3810 | 7.6370 | 90 | Orthorhombic |
| $x = 1.0$ | 5.4424 | 5.3807 | 7.6417 | 90 | Orthorhombic |

used as the internal standard for the calculation of the lattice parameters of the specimens. As shown in Table 1, the specimens with $x \leq 0.1$ could be indexed to rhombohedral structure. When $0.3 \leq x \leq 0.7$, the tetragonal structure was the more probable than any other model structure and it changed to orthorhombic structure as $x$ exceeded 0.7. It is worth to mention that according to the electron diffraction analysis, the cubic phase was found in the $0.1NdAlO_3$–$0.9CaTiO_3$ ceramics sintered at 1600°C. Since $CaTiO_3$ is cubic above 1327°C [18], a small amount of the high temperature cubic phase is considered to coexist with the orthorhombic phase in $0.1NdAlO_3$–$0.9CaTiO_3$ ceramics sintered at 1600°C. More detailed results on the crystal structure developed in $(1-x)NdAlO_3$–$xCaTiO_3$ ceramics will be published in the near future.

Fig. 2(a)–(e) show the SEM images of $(1-x)NdAlO_3$–$xCaTiO_3$ ceramics sintered at 1450°C for 6 h. The average grain size of specimens increased with the increase of $x$. Two types of second phases were also found in SEM images. For the specimens with $x \leq 0.5$, the second phase with needle shape was observed and it is considered

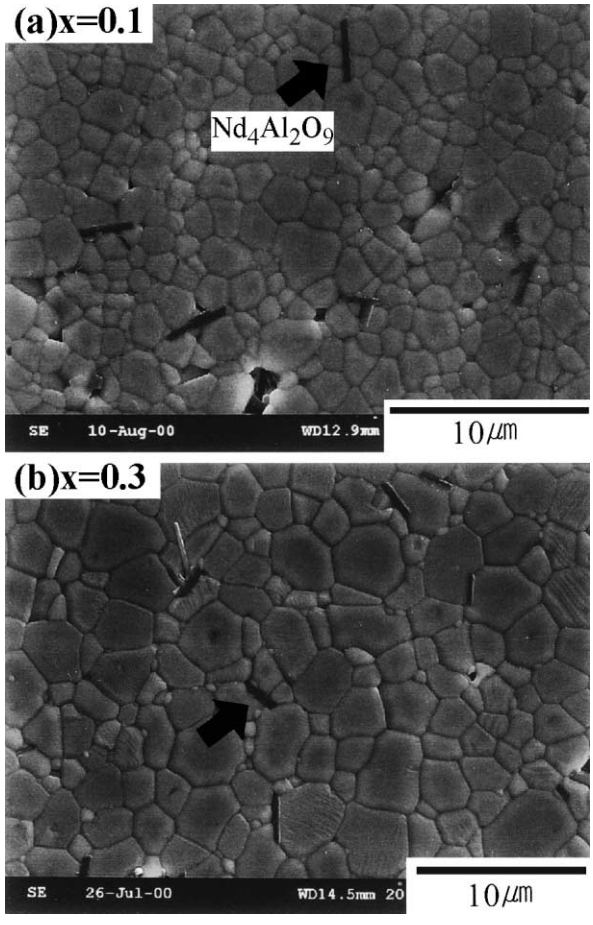


Fig. 2. SEM images of $(1-x)NdAlO_3$–$xCaTiO_3$ specimens sintered at 1450°C: (a) $x = 0.1$, (b) $x = 0.3$, (c) $x = 0.5$, (d) $x = 0.7$ and (e) $x = 0.9$.

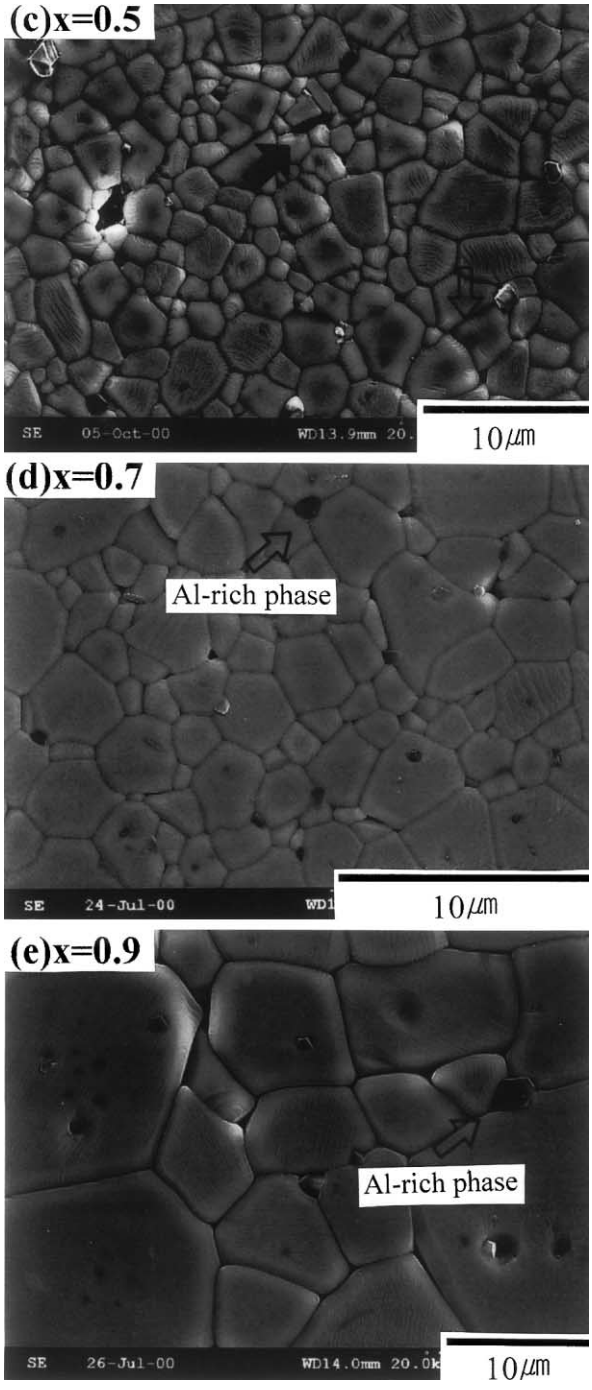


Fig. 2. (*Continued*).

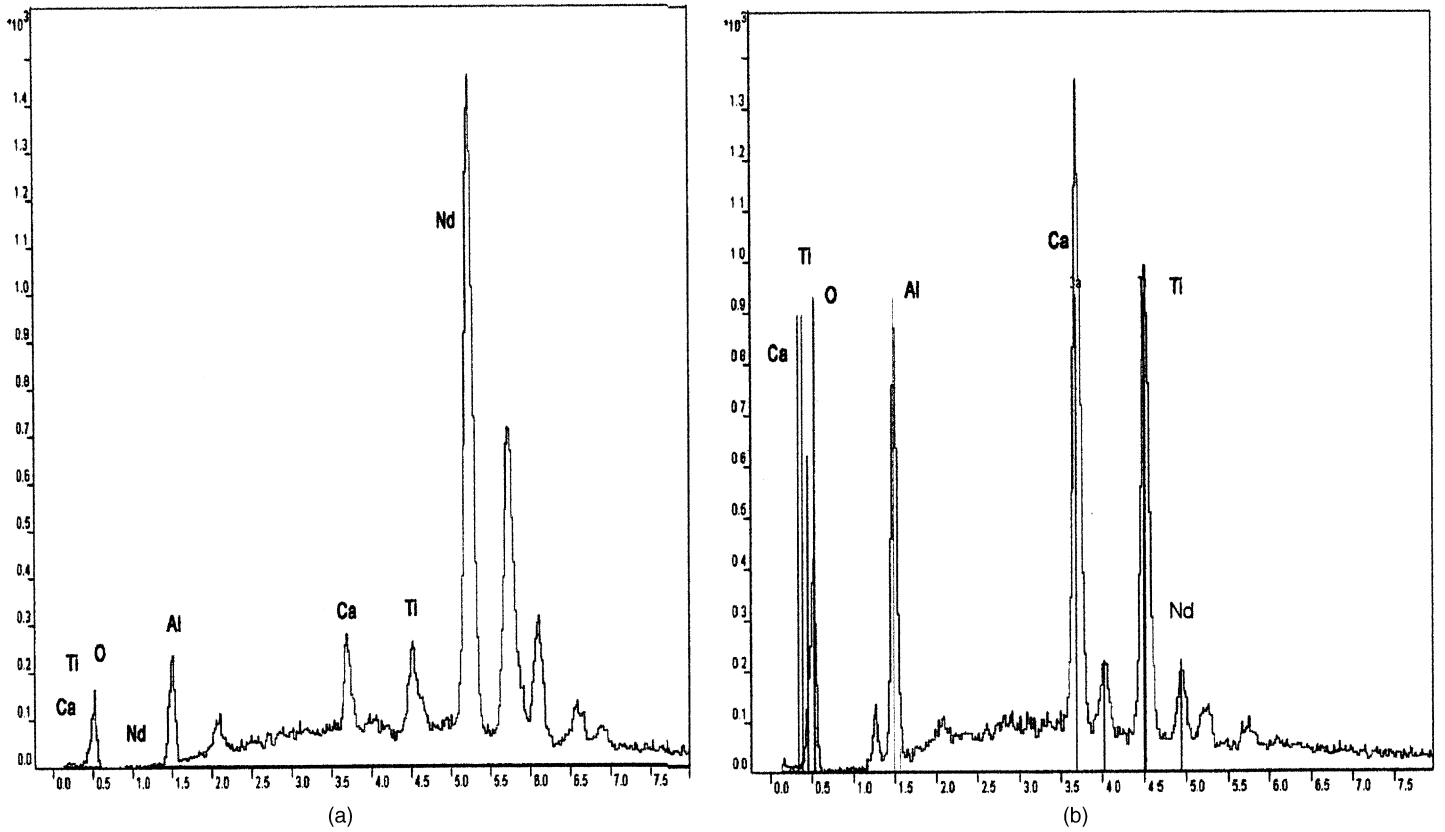


Fig. 3. EDS spectra of the second phases existed in (a) $0.9NdAlO_3$–$0.1CaTiO_3$ ceramics, and (b) $0.1NdAlO_3$–$0.9CaTiO_3$ ceramics.

as $Nd_4Al_2O_9$. For the specimens with $x \geq 0.7$, the second phase with the different shape was observed. In order to identify the composition of the second phases, EDS analysis was carried out on $0.9NdAlO_3$–$0.1CaTiO_3$ and $0.1NdAlO_3$–$0.9CaTiO_3$ ceramics. Fig. 3(a) illustrates the EDS spectrum of the second phase existed in $0.9NdAlO_3$–$0.1CaTiO_3$ ceramics. According to the quantitative analysis, the ratio of Al to Nd was about 0.5 and the amount of Ca and Ti was negligible. Therefore, this result confirms that the second phase formed in the specimens with $x \leq 0.5$ is $Nd_4Al_2O_9$. Fig. 3(b) shows the EDS spectra taken at the second phase found in the $0.1NdAlO_3$–$0.9CaTiO_3$ ceramics. Even though, the exact composition of the second phase was not identified, the high concentration of Al ions was found at the second phase. Therefore, the second phase formed in the specimens with $x \geq 0.7$ is the Al-rich phase.

Fig. 4 shows the variation of the relative density with $x$ for $(1-x)NdAlO_3$–$xCaTiO_3$ ceramics sintered at different temperatures. The relative densities of the specimens with $0.1 \leq x \leq 0.9$ were high ranged between 95 and 98% of the theoretical density. However, the relative density of $NdAlO_3$ ceramics sintered at 1450 or 1600°C was very low. Therefore, it is considered that $NdAlO_3$ ceramics is not completely sintered at 1450 or 1600°C. Fig. 4 also shows that the relative density of $0.1NdAlO_3$–$0.9CaTiO_3$ ceramics sintered at 1600°C is lower than that sintered at 1450°C. The density of the high temperature cubic $CaTiO_3$ phase is lower than that of orthorhombic phase [18,19]. Therefore, the low density of $0.1NdAlO_3$–$0.9CaTiO_3$ ceramics sintered at 1600°C could be explained by the presence of cubic phase. In addition, as shown in Fig. 5, the average grain size of the specimens with $x < 0.9$ sintered at 1600°C is slightly larger than that sintered at 1450°C. However, it suddenly

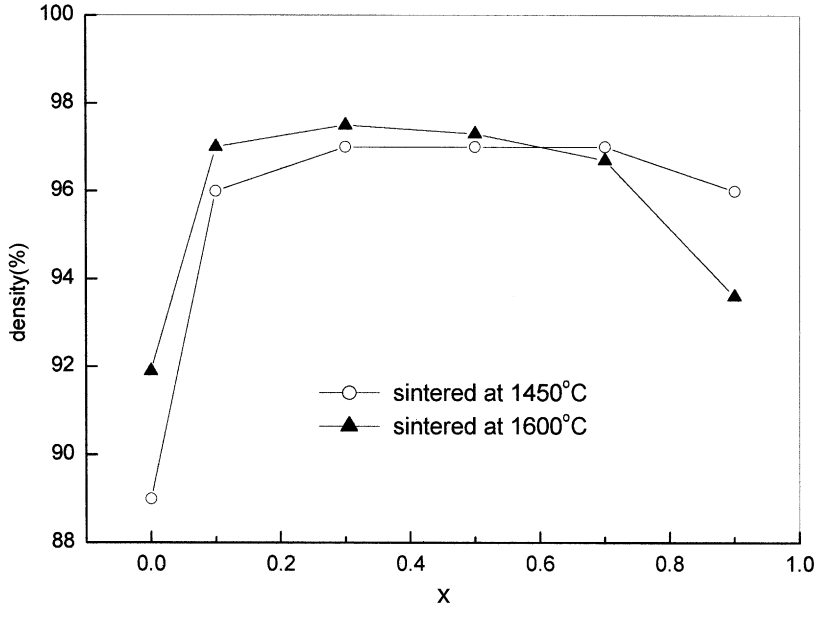


Fig. 4. Variation of the relative density with $x$ for $(1-x)NdAlO_3$–$xCaTiO_3$ ceramics.

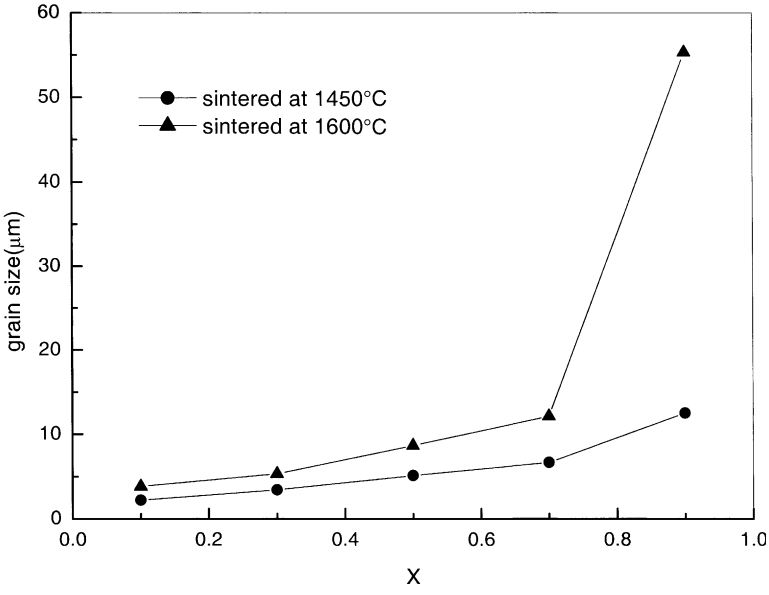


Fig. 5. Variation of the average grain size with $x$ for $(1-x)NdAlO_3$–$xCaTiO_3$ ceramics.

increased for $0.1NdAlO_3$–$0.9CaTiO_3$ ceramics sintered at 1600°C. Therefore, the sudden grain growth could be also responsible for the low density of $0.1NdAlO_3$–$0.9CaTiO_3$ ceramics.

The dielectric constant of $(1-x)NdAlO_3$–$xCaTiO_3$ ceramics with $0.0 \leq x \leq 0.9$ was illustrated in Fig. 6. It increased with $x$ but the rate of the increase varies with the composition and the structure. The change of the $\varepsilon_r$ was negligible for the specimens with $x \leq 0.1$ which have the rhombohedral structure. For the specimens with $0.3 \leq x \leq 0.7$ which have the tetragonal structure, $\varepsilon_r$ increased with $x$ but the rate of the increase was small. As $x$ exceeded 0.7, the tetragonal structure changed to the orthorhombic structure and the $\varepsilon_r$ increased significantly. The $\varepsilon_r$ of $0.3NdAlO_3$–$0.7CaTiO_3$ ceramics was about 45. In addition, the $\varepsilon_r$ of $0.1NdAlO_3$–$0.9CaTiO_3$ ceramics sintered at 1600°C is relatively low compared with that sintered at 1420 and 1450°C. It is probably due to the presence of the cubic phase, which decreased the density of the specimen. However, since the dielectric properties of the cubic phase have not been known, the effects of the cubic phase on the dielectric properties of the specimen are not completely understood at this moment.

Fig. 7 illustrates $\tau_f$ of the $(1-x)NdAlO_3$–$xCaTiO_3$ ceramics. The $\tau_f$ of $NdAlO_3$ ceramics was about $-50$ ppm/°C. The behavior of $\tau_f$ with $x$ was similar to that of the $\varepsilon_r$. The variation of $\tau_f$ was negligible when the specimen has the rhombohedral structure. For the specimens with $0.3 \leq x \leq 0.7$, $\tau_f$ of the specimen slowly increased with $x$. However, it greatly increased for the specimens with $x > 0.7$. The $\tau_f$ of $0.3NdAlO_3$–$0.7CaTiO_3$ was about $-1.5$ ppm/°C.

The variation of the $Q \times f$ value with $x$ for $(1-x)NdAlO_3$–$xCaTiO_3$ ceramics is shown in Fig. 8. According to the previous work, the $Q \times f$ value of $NdAlO_3$ ceramics

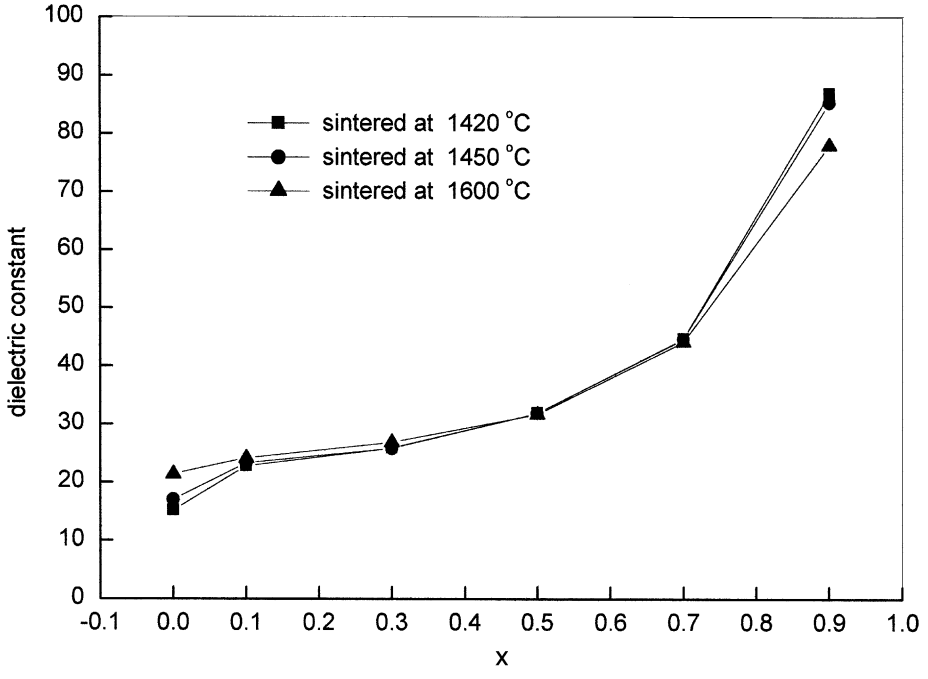


Fig. 6. Variation of the dielectric constant with $x$ for $(1-x)NdAlO_3$–$xCaTiO_3$ ceramics.

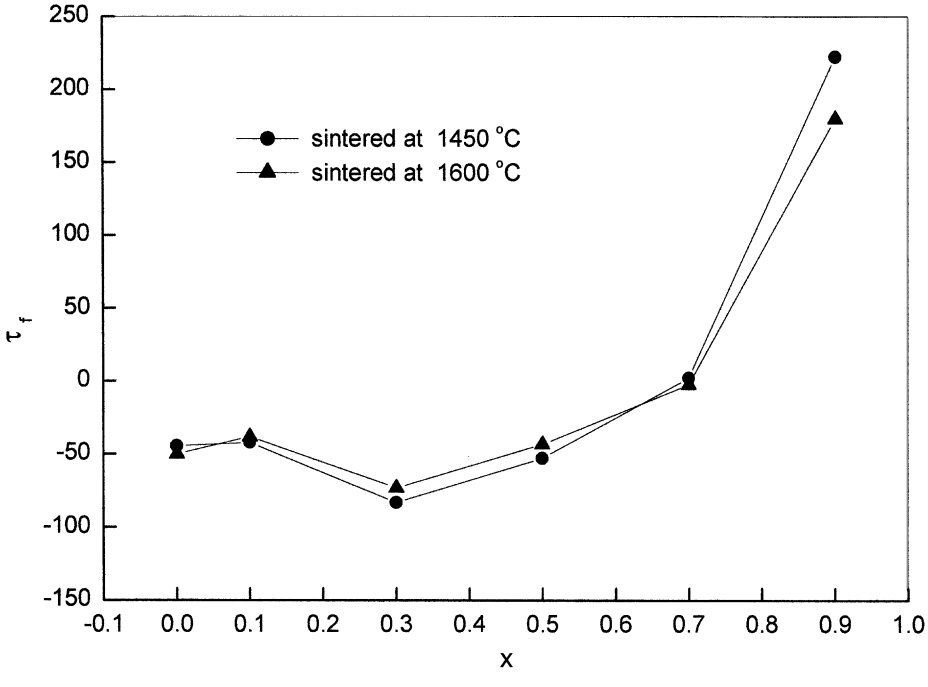


Fig. 7. Variation of the temperature coefficient of resonant frequency with $x$ for $(1-x)NdAlO_3$–$xCaTiO_3$ ceramics.

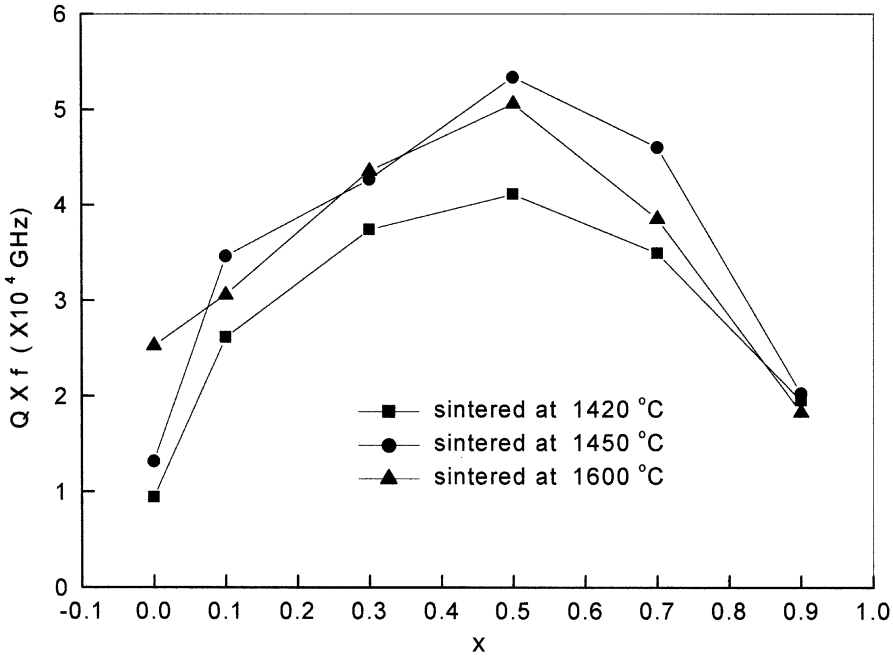


Fig. 8. Variation of the $Q \times f$ value with $x$ for $(1-x)NdAlO_3$–$xCaTiO_3$ ceramics.

is about 60,000 GHz [15]. Therefore, it was expected that $NdAlO_3$ has the highest $Q \times f$ value and it decreases with the increase of $x$ as found in $(1-x)LaAlO_3$–$xCaTiO_3$ system. However, the $Q$-value of $NdAlO_3$ was very low and it increased with $x$ and exhibited the maximum value as $x = 0.5$. This anomalous result could be explained by the presence of $Nd_4Al_2O_9$ second phase. As shown in Fig. 1, the $Nd_4Al_2O_9$ phase exists in the $NdAlO_3$ and the amount of $Nd_4Al_2O_9$ phase decreased with $x$. Therefore, the low $Q \times f$ value of the specimens with $x < 0.5$ is attributed to the presence of $Nd_4Al_2O_9$ phase. In addition, for $NdAlO_3$ ceramics, the low relative density is also responsible for the deterioration of $Q$-value. Fig. 8 also shows the variation of the $Q \times f$ value with the sintering temperature. The $Q \times f$ value of the specimens sintered at 1420°C was relatively low. However, for the specimens sintered above 1420°C, the variation of $Q \times f$ value with the sintering temperature was not significant. The $Q \times f$ value of $0.3NdAlO_3$–$0.7CaTiO_3$ ceramics sintered at 1450°C was about 45,000 GHz. Therefore, $0.3NdAlO_3$–$0.7CaTiO_3$ ceramics exhibited excellent dielectric properties and it can be a good candidate for the microwave dielectric materials.

## References

[1] K. Wakino, K. Minai, H. Tamura, J. Am. Ceram. Soc. 67 (4) (1984) 278.
[2] W. Wersing, in: B.C.H. Steele (Ed.) Electronic Ceramics, Elsevier, New York, 1991, p. 69 (Chapter 4).
[3] D. Kolar, Z. Stadler, S. Gaberscek, D. Suvorov, Ber. Dr. Keram. Ges. 55 (1978) 7.

[4] H. Oshato, J. Sugino, A. Komura, S. Nishigaki, T. Okuda, Jpn. J. Appl. Phys. 38 (1999) 5625.
[5] J. Kato, H. Kagata, K. Nishimoto, Jpn. J. Appl. Phys. 30 (1991) 2343.
[6] S. Nomura, K. Toyama, K. Kaneta, Jpn. J. Appl. Phys. 21 (1982) L624.
[7] S. Kawashima, M. Nishida, I. Ueda, H. Ouchi, Am. Ceram. Soc. 66 (1983) 421.
[8] S.B. Desu, H.M. O'Bryan, J. Am. Ceram. Soc. 68 (10) (1985) 546.
[9] G. Wolfram, H.E. Gobel, Mater. Res. Bull. 16 (1981) 1455.
[10] J.H. Moon, H.M. Jang, H.S. Park, J.Y. Shin, H.S. Kim, Jpn. J. Appl. Phys. 38 (1999) 6821.
[11] P. Sun, T. Nakamura, Y.J. Shan, Y. Inaguma, M. Itoh, T. Kitamura, Jpn. J. Appl. Phys. 37 (1998) 5625.
[12] S.Y. Cho, I.T. Kim, K.S. Hong, Jpn. J. Appl. Phys. 37 (1998) 593.
[13] D.H. Yeo, J.B. Kim, J.H. Moon, S.J. Yoon, H.J. Kim, Jpn. J. Appl. Phys. 35 (1996) 663.
[14] F.S. Gallaso, Structure, Properties and Preparation of Perovskite-type Compounds, Pergamon Press, Oxford, 1994.
[15] D.G. Lim, Ph.D. thesis, Korea University, South Korea, 1999.
[16] B.W. Hakki, P.D. Coleman, in: Proceedings of the IEEE Transactions on Microwave Theory. Tech. MTT-8, 1960, p. 402.
[17] W.E. Courtney, in: Proceedings of the IEEE Transactions on Microwave Theory. Tech. MTT-18, 1970, p. 476.
[18] JCPDS Diffraction Data Card No. 43-0226.
[19] JCPDS Diffraction Data Card No. 42-0423.